Concurrent optimisation of brain states and behavioural strategies when learning complex tasks

Richard E. Daws[1], Gregory Scott[1], Eyal Soreq[1], Robert Leech[2], Peter J. Hellyer[2] & Adam Hampshire[1].

[1]The Computational, Cognitive and Clinical Neuroimaging Laboratory (C[3]NL), Imperial College London, UK.

[2]Department of Neuroimaging, Institute of Psychiatry, Psychology and Neurosciences, King's College London, London, UK.

Abstract

We designed two novel fMRI paradigms to investigate how people self-optimise performance when managing competing demands. We hypothesised that the brain adopts distinct functional states to support different tasks, that switching between them involves a costly process of collapse and reconfiguration of the functional connectome, and that this process is optimised with practice. Accordingly, self-ordered switches (SOS) were associated with transient states of low-connectivity and high-activation. Individuals progressively improved their performance with practice. This learning behaviour was reflected by an ongoing redeployment of the neural resources supporting switching and routine behaviour. Furthermore, those who developed more structured behaviours also scored more points, showed a greater deepening of switching-dysconnectivity and a greater tuning of activity within dorsal frontoparietal cortex to switching events with practice. These results demonstrate that a fundamental property of human neurocognitive systems is concurrent self-optimisation to maximise behavioural outcomes and minimise the use of neural resources.

Keywords: Cognitive control, structured behaviours, task-switching, learning, fMRI.

Task-switching paradigms have been used for over a century to study how humans redeploy their attention between tasks [1,2]. The requirement to switch results in individuals responding more slowly than they would when performing repeated trials of the same task. This difference in response speed between switch and repeat trials is the "switch cost". Switch costs are amongst the most replicated findings in cognitive neuroscience [1–11]; however, our understanding of the underlying neural mechanisms remains rudimentary at best, and lacks ecological validity [9,11,12].

A major limitation in our understanding relates to the fact that experimental tasks are typically designed to explicitly control when the switching events occur [12]. Conversely, in everyday life, people often structure their behaviours and *choose* when to switch. Some studies have attempted to address this by developing paradigms where individuals randomly volunteer when to task-switch [10,13–15]. However, these paradigms fail to capture the natural inclination to apply structure to behaviour [16,17] and to optimise behavioural strategies through learning [18–23]. Indeed, the self-organisation of switching is evident without prior instruction, even when there is no explicit behavioural benefit from a computational perspective [17]. This prominent characteristic of human behaviour provides an intriguing perspective of cognitive dysfunction, because some neurological populations exhibit a marked paucity of structure when performing new tasks [17,24,2526]. This behavioural disorganisation is likely a characteristic of cognitive impairments that impacts on daily life [26,27].

A further limitation is that functional MRI (fMRI) studies of task-switching have historically focused on identifying one-to-one mappings between task-switching and functional activation in specific brain regions. The locus of reported activation varies, but the anterior prefrontal cortex (aPFC) [28–30] is a recurring theme. This mapping is supported by observations from classic neuropsychology (e.g. executive dysfunction following aPFC lesions [31–34]) and the widely-held perspective that regions within aPFC are arranged along an abstract-concrete anterior-posterior axis [35,36]; subsequently, activation in the (most-anterior) frontopolar cortex during task-switching is explainable as switching is considered an exemplar of a high-abstraction process [8,28–30].

However, such one-to-one mappings may not capture the dynamic brain mechanisms that support cognition and organise behaviour [37–40]. Conversely, the contemporary network science view proposes that cognitive controls are fundamentally non-localisable because they are supported by dynamic interactions that occur across distributed networks of brain regions [20,22,41–50]. Indeed, *distributed* activations, including aPFC, can occur during task-switching [8,51–

[56], instruction based learning (IBL) [20,21,26], relational integration [46] and even during tasks that lack overt requirements for abstraction or hierarchy in cognitive processing [57]. Moreover, we have shown that activation in aPFC decays along an anterior-posterior axis as individuals overcome novelty and automate behaviour [20,21,26]. Together, these results converge on the alternate view that anterior portions of aPFC are recruited as part of a wider functional network during demanding tasks in general [58,59].

More broadly, network neuroscience studies of cognitive control demonstrate that when engaging with a task there is a substantial reorganization of the brain's functional connectome [49,60,61], characterised by the transition from a state of high-activation to a low-activation high-connectivity state [18–23,62], and this transition rate may depend on learning. Critically, the established task-state expresses a stable [44,62] connectivity pattern that is specific enough to the task [22,47,50,63–65], cognitive load [22], performance [66] and clinical abnormalities [67–69] to be decoded with machine learning.

Here, we developed two "self-ordered switching" (SOS) paradigms to address the aforementioned limitations of ecological validity and the opposing modular and dynamic-network models of cognitive control. Across two independent fMRI studies, individuals' SOS behaviour was either guided by hierarchical feedback (study 1), or by a task program that was learnt during a pre-training session (study 2).

We first tested the hypothesis that switching between tasks requires a costly process of collapse and reconfiguration of the brain's functional connectome (Figure 1). In doing so, we directly tested for evidence of a modular hierarchy within aPFC or a dynamic-network process that supports switching behaviours. The former would be supported by evidence of strong switching-activation in anterior PFC (e.g., frontal poles), with this being strongest during task-switching relative to rule-switching. The latter would be supported by evidence of highly distributed changes in connectivity and activation during switching.

Next, we tested the hypothesis that the brain regions that support switching behaviour vary as a function of learning. From a dynamic-network perspective, we predicted that neural resources would tune towards the demanding switch events as the simple trial responses became automated with learning. Finally, we quantified individuals switching behaviour using algorithmic complexity [70] to examine how behavioural structure facilitates the optimisation of neural resources during the performance of complex tasks.

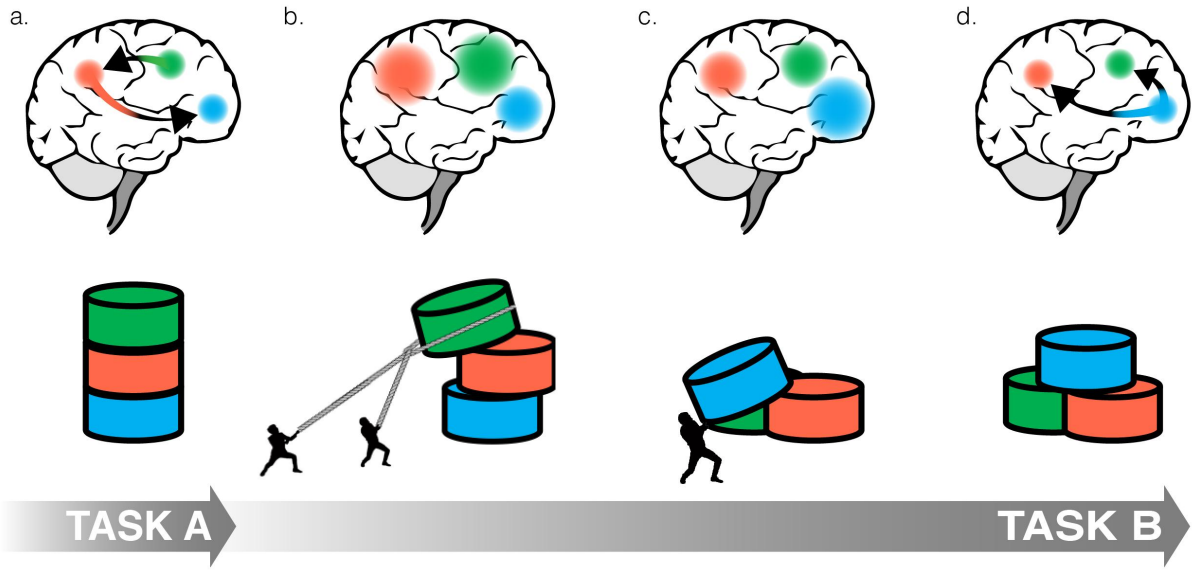

Figure 1. **Schematic of hypothesised task-switching reconfiguration in the brain.** Distinct tasks can recruit similar brain regions, but distinct patterns of activation and hierarchical connectivity. a) In this hypothetical example, "TASK A" is supported by a pattern where the green region drives the activities of the red region which drives the blue region, in turn. This stable state is represented as a stack, below. b) During a task-switch from TASK A to TASK B, activation increases as the outgoing connectivity state is destabilized and reconfigured (c) to support the incoming TASK B demands. d) This process resolves with TASK B being supported by a connectivity state where the blue region drives the activities of both green & red regions equally.

Results

We designed two novel paradigms that required participants to self-organise their time on either a matching task (MT) or an odd one out (OOO) task. Each task had two visual discrimination rules, colour and shape, and on each trial, the participants performed a discrimination according to one of these rules (Figure 2a). The discrimination rules were simple enough to be performed at high accuracy with minimal effort. This ensured that individuals focused on dividing their time across the tasks and rules to gain maximum points.

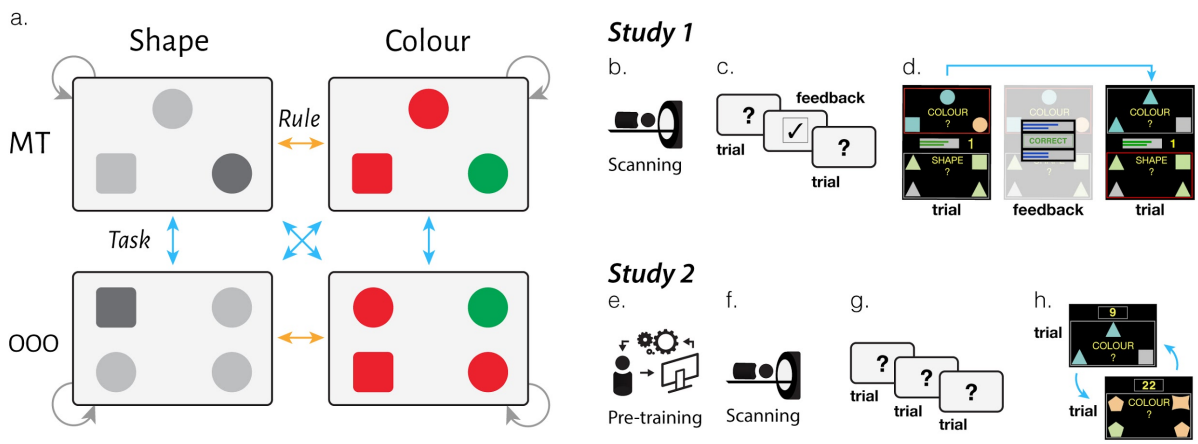

Figure 2. **Self-ordered switching (SOS) paradigms.** a) Schematic of the two tasks (MT - Matching task, OOO - Odd one out) and the two rules (colour, shape) in each row and column, respectively. Arrows represent possible sequences of trials and switches that could be performed by an individual: Repeat trials (grey) and switches between rules (orange) or tasks (blue). b) Study 1 involved a 20 minute fMRI session where subjects performed SOS that was guided by hierarchical response feedback (c). d) An example of a MT -> OOO task-switch following feedback. Each task was displayed simultaneously with the active task being denoted by a red border. Feedback was hierarchical with correct responses accumulating progress on one the blue bars, where each bar represented one of a task's sub-rules. By balancing time on both sub-rules from a given task progress the green bar for that task and balancing time on both tasks lead to an increase in the overall score. e) Study 2 involved an additional pre-training session prior to scanning (f) where SOS was performed in the absence of response feedback. h) This SOS paradigm also differed in that tasks were shown individually.

Study 1: Feedback guided SOS. While in the MRI scanner, 16 healthy individuals performed SOS for 20 minutes while being guided by response feedback (Figure 2b-d). Visual discriminations were made on each trial using left or right button presses. Switches between tasks and rules were made using up or down button presses. Response feedback occurred after each trial and consisted of a set of hierarchically organised meters and an overall score. Each task had an overall progress meter, and two subordinal meters corresponding to the discrimination rules. To increment the task meters, both rule meters for that task had to progress, which occurred when a correct response was made for a corresponding trial. To score maximum points, both task meters had to progress. Response errors, or making too many responses on a particular rule or task, resulted in penalties that hindered progress (see

methods). Thus, those who learnt the most efficient strategy of responding to trials and switching, via trial and error, should accumulate the most points during the experiment.

Response speed costs reduce with learning. To test for behavioural switch costs, median reaction times (RT) for repeat trials were compared to those trials that followed task-switching or rule-switching (Figure 3a). RT significantly varied across condition (one-way repeated-measures analysis of variance: $F_{2,30}$=48.588, p<0.001, η_p^2=0.76). Relative to repeat trials, average response speeds for task-switching slowed by 883ms (SD=538) (paired t-test: t_{15}=6.573, p<0.001, confidence interval 95% (CI)=0.54 to 1.17, Cohen's *d*=1.64), and rule-switches were 179ms (SD=273) faster (t_{15}=-2.630, p=0.019, CI=0.03 to 0.33, *d*=0.66). Response accuracy did not vary across condition (one-way rm-anova: $F_{2,30}$=1.218, p=0.310, η_p^2=0.08) and was near-ceiling across individuals (mean=94.87%, SD=4.18). Thus, SOS costs were specific to response speed.

We then examined how RT switching costs varied as individuals practised SOS (Figure 3b-c). Those who performed more switches were faster to respond after switching (pearson: r_{15}=-0.557, p=0.025, CI=-0.83 to -0.09). Examining within-subject learning across three time-windows (~7 minutes), task-switching costs varied with practise (one-way rm-anova: $F_{2,30}$=3.579, p=0.040, η_p^2=0.19) and reduced by ~370ms (SD=607) between the first and last time-window, on average (paired t-test: t_{15}=-2.433, p=0.028, CI=45.68 to 692.54, *d*=0.52). Rule-switching costs did not vary with practise ($F_{2,30}$=0.128, p=0.881, η_p^2=0.01).

Structuring behaviour increases efficiency. Individuals' behavioural strategies were quantified using algorithmic complexity [70], a measure (quantifying the length of the shortest algorithm that can produce a sequence) that is greater for random sequences, vs. sequences with consistent structures. Algorithmic complexity strongly related to the number of points scored by each individual, their efficiency (partial correlation, factoring N-trials: r_{15}=-0.646, p=0.017, CI=-0.87 to -0.22) as those who applied more structure to their switching behaviour scored more points (Figure 3d). For clarity, behavioural timecourses from low-, medium- and high-performers are displayed in Figure 3e. Critically, individuals' scores did not relate in a trivial manner to the number of switches between tasks (pearson: r_{15}=0.213, p=0.428, CI=-0.32 to 0.64) or rules (r_{15}=0.473, p=0.065, CI=-0.03 to 0.79). This demonstrates that applying sequential structure helps people to efficiently organise their behaviour during complex tasks.

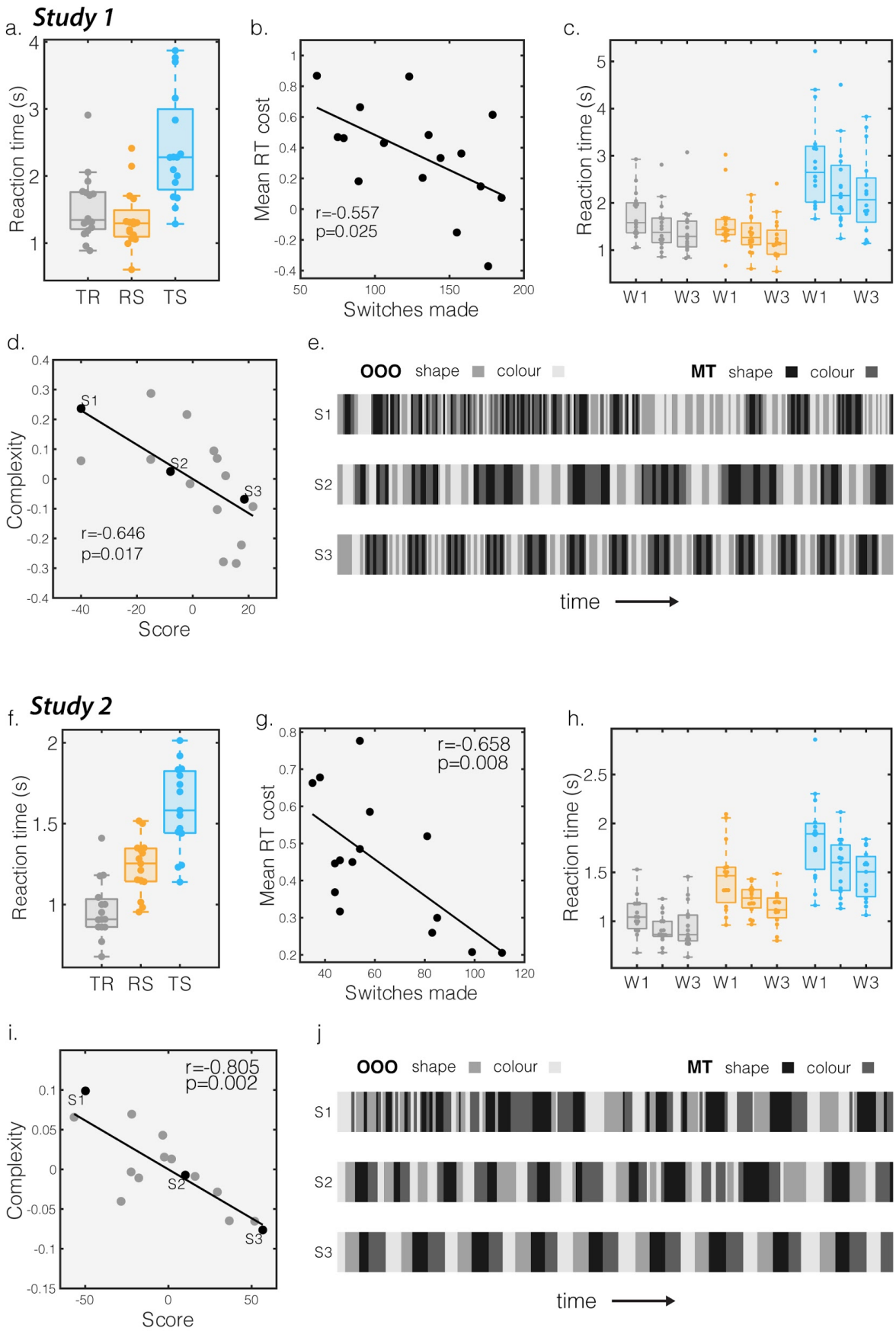

Figure 3. **Switching costs to response speed reduces with practise and efficiency relates to structured behaviour.** Study 1 - a) Individuals median reaction time (RT) in seconds (s) for repeat trials (TR - grey) and trials following a rule-switch (RS - orange) or task-switch (TS - blue). Central line of the boxplots refer to

the group median, top and bottom edges of the box represent the 25th and 7th percentile, respectively. Data beyond the whiskers are outliers. b) The mean task-switch and rule-switch cost to RT negatively correlates with the total number of switches made. c) Median RT from 3 ~7 minute time-windows (W) for TR, RS and TS. d) Individuals algorithmic complexity negatively correlated with overall task score (plotting the residuals from a partial correlation that factored out the number of trials completed). Labelled darker datapoints refer to individuals whose behavioural timecourses are depicted in e. e) The sequence of trials performed by three individuals with high, average and low algorithmic complexity. Study 2 - f-j) Data analysis and visualisation procedure repeated for study 2.

Dysconnectivity during SOS. Next we examined how SOS perturbs the brain's functional organisation by estimating dynamic functional connectivity (dFC), with generalised psychophysiological interactions (gPPI) [71,72], to each pair of mean fMRI timecourses from 159 cortical, subcortical and cerebellar regions of interest (ROI) [73–75]. This produced an nROI x nROI x nCondition matrix of dFC estimates for each individual that were then z-scored across condition. Each dFC estimate represents the *change* in FC for a specific connection dependent on the condition of interest; this was relative to that connection's baseline FC for that individual.

The distribution of task-switching dFC (all connections and individuals) was significantly reduced, compared to trial response dFC (Kolmogorov-Smirnov: ks=0.665, $p<0.001$; paired t-test: $t_{4.019e+5}$=-725.797, $p<0.001$, CI=1.225 to 1.232, d=1.80, (Figure 4a). The same pattern was observed when repeating this procedure for rule-switching (ks=0.746, $p<0.001$; $t_{4.019e+5}$=-1.161e+03, $p<0.001$, CI=1.079 to 1.083, d=2.32). Comparing individuals' average dFC change (across connection) during switching against 0 demonstrated that this dysconnectivity effect was consistent across individuals for task-switching (one-sample t-test: t_{15}=-10.403, $p<0.001$, CI=-1.48 to -0.98, d=2.60) and rule-switching (t_{15}=-20.495, $p<0.001$, CI=-1.19 to -0.97, d=5.12, Figure 4b).

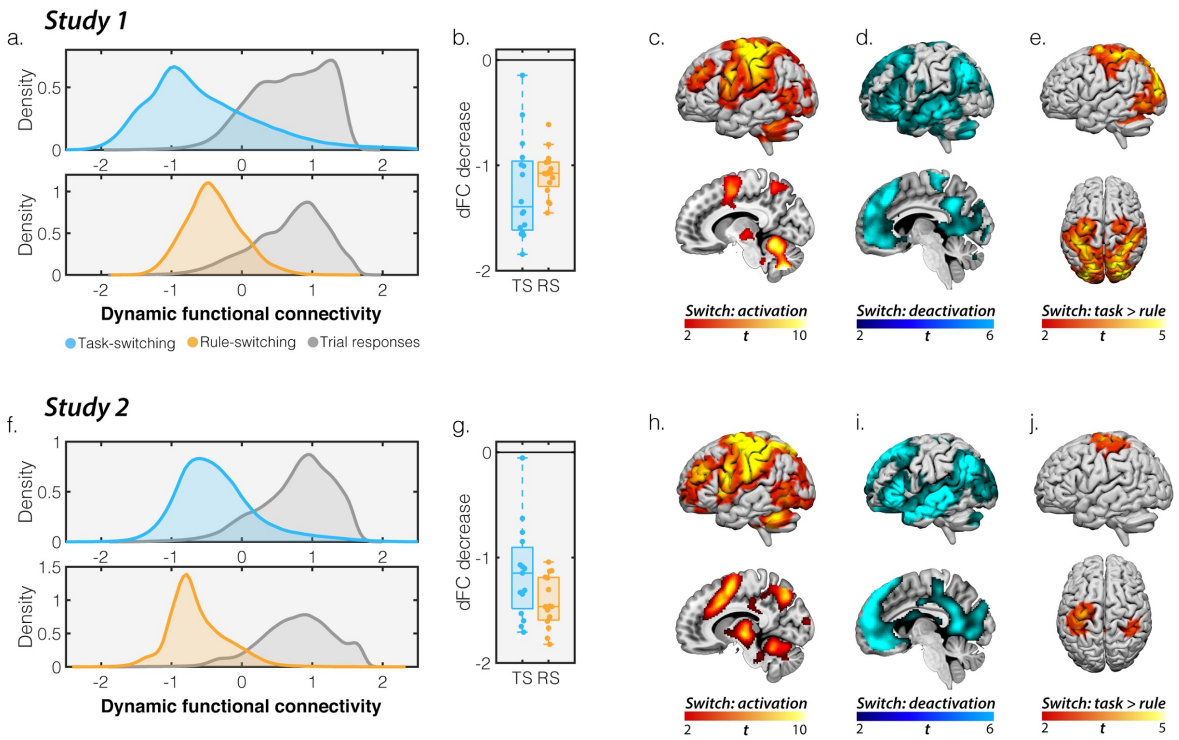

Figure 4. **Widespread reductions in functional connectivity during switching are accompanied by lateral frontoparietal activation and default mode deactivation.** Study 1 - a) Distributions of dynamic functional connectivity (dFC) weights from all connections and individuals, z-scored across condition (within-individual). Top row - Mean task-switching (TS, blue) dFC compared to mean trial dFC (grey, collapsed across rule). Bottom row - Mean rule-switching (RS, orange) dFC compared to mean trial dFC (collapsed across task). b) The mean difference in dFC between TS and trials (blue) and between RS and trials (orange) across all connections, for each individual. Central line of the boxplots refers to the group median, top and bottom edges of the box represent the 25th and 7th percentile, respectively. Data beyond the whiskers are outliers c) T-contrast maps rendering significant increases (c) and decreases (d) in activation. e) T-contrast testing for significantly greater activation for task>rule-switching. There were no significant clusters when testing the inverse rule>task-switching contrast. All statistical maps are thresholded at an uncorrected $p<0.01$ followed by a $p<0.05$ FDR cluster-correction. Study 2 - f-j) Data analysis and visualisation procedure repeated for study 2.

SOS activates lateral frontoparietal cortex and deactivates the default mode network. We next captured changes in functional activation during switching using whole-brain voxelwise contrasts modelled with a one-way rm-anova (6 levels). Activation increases occurred in a broad set of dorsolateral frontoparietal and cerebellar cortices, and also in the insula, putamen, and thalamus (Figure 4c). Concurrently, deactivation occurred (Figure 4d) in dorsomedial frontoparietal and temporal cortices, a distribution of activity resembling the default mode network (DMN). Contrasting activation during task-switching and rule-switching rendered increases in the dorsal visual streams and frontal eye fields (Figure 4e) during task-switching. No region showed activation during rule-switching that was greater for task-switching.

Frontoparietal & occipital activation during visual discriminations. Modelling activation with a task (MT, OOO) by rule (colour, shape) rm-anova, indicated a bilateral pattern of

dorsolateral frontoparietal and occipital cortex activation during trial responding (Supplemental figure 1a). Testing for the main effects of task and rule produced clusters in occipital cortices (Supplemental figure 1b-c); comparing their mean activation showed greater activation during OOO, relative to MT (paired t-test: t_{15}=9.618, p<0.001, CI=0.84 to 0.54, *d*=0.86), and greater activation for colour, relative to shape trials (t_{15}=7.928, p<0.001, CI=0.23 to 0.40, *d*=0.34).

Study 2: SOS without feedback, internally guided. Study 1 demonstrates that SOS costs reduce with learning and structuring behaviour increases efficiency. We also presented evidence supporting the hypothesis that SOS is facilitated by widespread dysconnectivity and activation changes in the brain that are not specific to aPFC. A pertinent question is whether the same relationships between switching behaviour and network dynamics are evident in the absence of feedback. To address this, we sought to replicate these findings in an independent fMRI study (n=15) using a variant of the SOS paradigm where behaviour was guided by the strategy that had been learnt based on hierarchical feedback during a pre-training session, with only the overall score presented during the scanning session itself (Figure 2e-h). As a further control, the two tasks were presented individually in the centre of the screen, that is, as opposed to in parallel at the top and the bottom of the screen, to control for spatial switching.

Switch costs reduce with learning & structuring behaviour increases efficiency: internally guided SOS. Replicating study 1, RT varied across repeat and switch trials (one-way rm-anova: $F_{2,28}$=52.886, p<0.001, η_p^2=0.79, Figure 3f). On average, response speed slowed by 267ms (SD=143) after rule-switching (paired t-test: t_{14}=7.214, p<0.001, CI=0.19 to 0.35, *d*=1.86), and was even slower after task-switching (t_{14}=5.227, p<0.001, CI=0.21 to 0.51, *d*=1.35) by 362ms (SD=268). Response accuracy did not differ across condition ($F_{2,28}$=1.867, p=0.173, η_p^2=0.12) and was near-ceiling (mean=94.69%, SD=4.04).

Those who switched more often were faster after switching (pearson: r_{14}=-0.658, p=0.008, CI=-0.88 to -0.22, Figure 3g), and costs varied with practise (Figure 3h) for task-switching (one-way anova: $F_{2,28}$=5.413, p=0.010, η_p^2=0.28) and rule-switching ($F_{2,28}$=5.543, p=0.009, η_p^2=0.28). Between the first and last time-windows, costs reduced by ~280ms (SD=418) for task-switching (paired t-test: t_{14}=-2.570, p=0.023, CI=45.94 to 509.33, *d*=0.81), and by ~220ms (SD=286) for rule-switching (t_{14}=-2.945, p=0.011, CI=59.04 to 375.46, *d*=0.88), on average. Algorithmic complexity showed a strong relationship with task performance, with those applying more structure scoring more points (partial: r_{14}=-0.805, p=0.002, CI=-0.93 to -

0.50, Figure 3i-j) and complexity did not correlate with the number of task-switches (pearson: r_{14}=0.034, p=0.905, CI=-0.49 to 0.54) or rule-switches (r_{14}=0.160, p=0.569, CI=-0.38 to 0.62).

Dysconnectivity, lateral frontoparietal activation and DMN deactivation during internally guided SOS. The dFC analyses of internally guided SOS replicate the switching-dysconnectivity observed in study 1. The dFC distribution (Figure 4f) was significantly reduced during task-switching (ks-test: ks=0.715, p<0.001; paired t-test: $t_{3.769+e5}$=796.025, CI=1.142 to 1.148, *d*=2.08) and rule-switching (ks=0.849, p<0.001; $t_{3.769+e5}$=1.261+e3, p<0.001, CI=1.417 to 1.422, *d*=3.03). The average dFC change across connections was also consistent across individuals (one-sample t-test: task-switching, t_{14}=-10.029, p<0.001, CI=-1.39 to -0.90, *d*=2.59; rule-switching, t_{14}=-22.386, p<0.001, CI=-1.56 to -1.28, *d*=5.78, Figure 4g).

Activation results (Figure 4h-i) were spatially consistent with study 1 for switching, with widespread increases in dorsolateral frontoparietal, subcortical and cerebellar regions (dice similarity coefficient: DSC=0.580) and DMN deactivation (DSC=0.562). However, comparing task-switching to rule-switching activation rendered a spatial pattern that differed to study 1, with activation localised to the motor cortices (DSC=0.210, Figure 4j). No region showed increased activation for rule-switching, compared to task-switching.

Frontal & occipital activation during visual discriminations. When activation for trials was modelled for study 2, activation was rendered in lateral frontal and occipital regions in a spatial pattern that had modest similarity with study 1 (DSC=0.270, Supplemental Figure 1d). However, the main effects of task (DSC=0.539, Supplemental Figure 1e) and rule (DSC=0.447, Supplemental Figure 1f) rendered occipital activation, with moderate spatial similarity to study 1, which varied across condition in a consistent manner to study 1 (OOO>MT (paired t-test: t_{14}=6.973, p<0.001, CI=0.63 to 0.34, *d*=0.87) and colour>shape (t_{14}=7.626, p<0.001, CI=0.20 to 0.36, *d*=0.59)).

SOS paradigm affects behavioural strategy. Having replicated the main findings from study 1, we next sought to directly compare the SOS studies to examine the effect of paradigm design on individual's behaviour. Individuals in Study 1 (feedback-guided) were less likely to repeat trials (two-sample t-test: t_{29}=-6.643, p<0.001, CI=-0.36 to -0.19, *d*=1.53, Figure 5a). The number of trial and switch events (Figure 5b) showed a significant interaction with study (two-way rm-anova: $F_{2,58}$=62.128, p<0.001; η_p^2=0.68). Specifically, study 1 individuals performed fewer trials (two-sample t-test: t_{29}=-5.262, p<0.001, CI=-81.87 to -36.04, *d*=1.38), but more

rule-switches (t_{29}=8.125, p<0.001, CI=49.85 to 83.39, *d*=1.64) than study 2 individuals and task-switches did not differ between studies (t_{29}=0.024, p=0.981, CI=-11.426 to 11.69, *d*=0.01).

Further, the ratio of task-to-rule-switching differed (two-sample t-test: t_{29}=-8.118, p<0.001, CI=-0.71 to -0.43, *d*=1.64), with study 1 individuals (mean=0.294, SD=0.139) more likely to switch within-task than study 2 (mean=0.865, SD=0.242), who performed task-switching or rule-switching almost equally (Figure 5c-d). Figure 5f-g visualises these behavioural differences with graphs weighted by the mean probability of one event following another in each study.

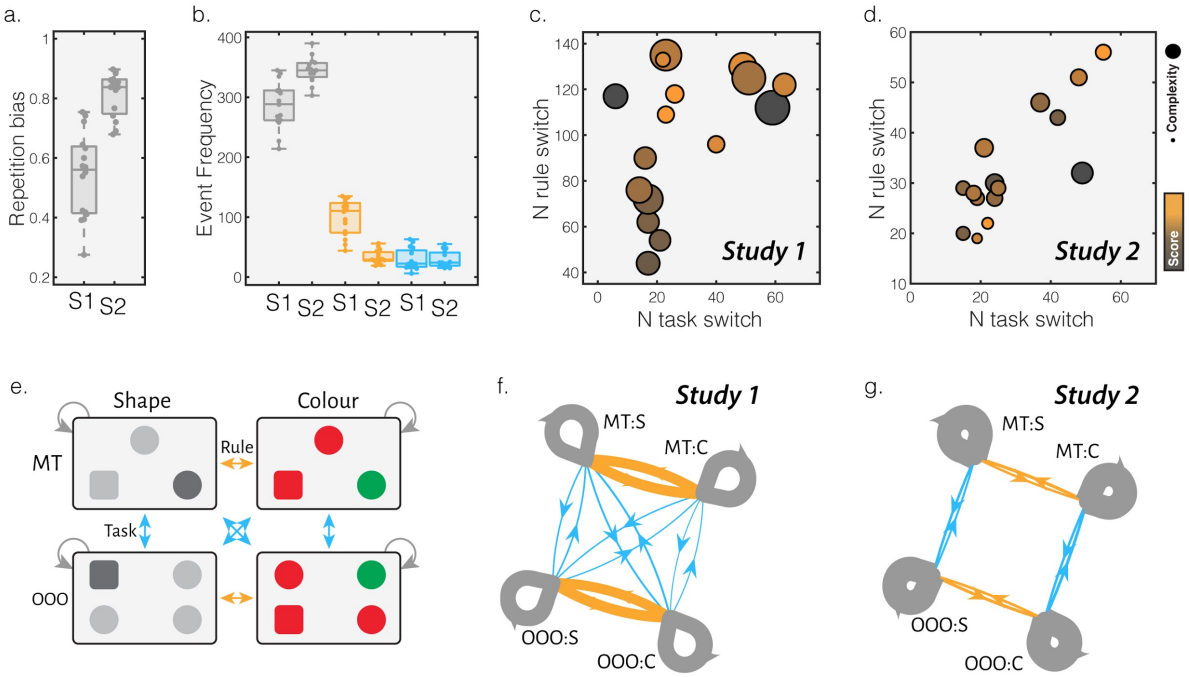

Figure 5. **Behavioural strategy differs across SOS paradigms.** a) The feedback guided SOS paradigm used in study 1 (S1) promoted a significantly lower repetition bias than the SOS paradigm in study 2 (S2). b) The number of events completed by subjects across studies (trials - grey, rule-switches - orange, task-switches - blue). c-d) Individual's number of task & rule-switches weighted by score (colour) & algorithmic complexity (diameter). Warm colours and small diameters represent high scoring individuals who applied more structure to their behaviour. e) Schematic of the two tasks (MT - Matching task, OOO - Odd one out) and the two rules (colour, shape) in each row and column, respectively. f-g) Graphs that represent the probability of one trial condition following another. Line thickness (edges) are weighted by the study mean proportion of trial repeats (grey), rule-switches (orange) and task-switches (blue). (C - colour, S - shape).

Switching dysconnectivity increases with learning and is maximised when behaviour is structured. Summarising these differences in behavioural strategies, algorithmic complexity was significantly lower in study 2 (two-sample t-test: t_{29}=4.500, p<0.001, CI=0.14 to 0.36, *d*=1.26, Figure 6a); suggesting that behaviour was more structured. We next

combined and compared the imaging data from both studies to test whether the structuring of behaviour affects the redeployment of neural resources that accompany learning during SOS.

FMRI data were modelled with three time-windows and switching-related dFC was extracted from each window. A two-way rm-anova, modelling time-window and study, showed that switching-dysconnectivity varied with learning stage ($F_{2,58}$=9.991, p<0.001, η_p^2=0.26) and study ($F_{1,29}$=18.751, p<0.001, η_p^2=0.39), but these factors did not interact ($F_{2,58}$=0.484, p=0.619, η_p^2=0.02). Combining both studies, switching-related network dysconnectivity *deepened* as the task was practiced, with dFC reductions during switching significantly greater in the last window, compared to the 1st (paired t-test: t_{30}=2.836, p=0.008, CI=-0.24 to -0.04, *d*=0.51). Building on this combined result, we examined how learning influenced the magnitude of switching-related dysconnectivity by summing the mean dFC change during switching across the three time-windows. This showed that individuals in study 2 had a significantly greater deepening of switching-dysconnectivity with learning (two-sample t-test: t_{29}=4.330, p<0.001, CI=0.33 to 0.91, *d*=1.23, Figure 6b). Combining data from both studies, larger increases in switching-related dysconnectivity related to increasingly structured behaviours (pearson: r_{30}=0.489, p=0.005, CI=0.16 to 0.72, Figure 6c).

Greater redeployment of neural resources during learning when behaviour is structured. Previous studies have reported decreased frontoparietal activation when simple tasks are established through practice [18,20,21]. To determine whether the same relationship is evident for complex tasks, learning-related changes in switching activation were modelled by comparing switch>trial voxelwise contrasts across time-window and study in a 3 * 2 rm-anova. *T*-contrasts examining the main effect of study showed overall greater switch > trial contrast in study 1 for the hippocampus and DMN and lower contrast in frontoparietal cortices, compared to study 2 (Supplemental Figure 1g).

The main effect of time-window *F*-contrast rendered bilateral clusters where switching-activation varied over time-window. Contrary to past studies, comparing the first and last time-windows, switching-activation *increased* (Figure 6d) in dorsolateral parietal cortex (DLPC - paired t-test: t_{30}=4.657, p<0.001, CI=1.65 to 0.64, *d*=1.56), anterior cingulate cortex (ACC - t_{30}=5.267, p<0.001, CI=1.37 to 0.61, *d*=1.59) and in occipital cortex (Occ. - t_{30}=4.707, p<0.001, CI=1.42 to 0.56, *d*=1.57). Using a “multiple-demand” composite from these three ROIs allowed us to examine the relationship between the sum of activation increase across time-window and individual’s algorithmic complexity (Figure 6e). The negative correlation between these

variables suggest that those who apply greater structure to their behaviour exhibit greater increases in multiple-demand activation with practise (pearson: r_{30}=-0.523, p=0.003, CI=-0.74 to -0.21). To help understand why this practise effect was inverted, relative to previous studies, we independently examined trial response activation, as these events are more comparable to simple learning curve paradigms [20,21]. Directly replicating these studies, activation in the multiple-demand ROI varied with learning (one-way anova: $F_{2,58}$=15.553, p<0.001, η_p^2=0.35) and was significantly decreased in the last window, compared to the first (paired t-test: t_{30}=-4.573, p=0.001, CI=-0.99 to -0.38, *d*=0.77, Figure 6f).

Repeating this procedure, but focusing on switching-activation *decreasing* over time-window (Figure 6g), three bilateral ROIs showed significantly reduced activation in the last window, compared to the first: The posterior cingulate cortex (PCC - t_{30}=-4.097, p<0.001, CI=-0.93 to -0.31, *d*=1.34), putamen (Put. - t_{30}=-3.412, p=0.002, CI=-0.91 to 0.23, *d*=1.14) and temporal cortex (Tem. - t_{30}=-5.401, p<0.001, CI=-1.12 -0.51, *d*=1.77). This pattern is also contrary to results reported when simpler tasks are being learnt [20,21]. NB:- All comparisons of the increasing and decreasing ROIs survive Bonferroni correction, n=6, alpha=0.05/n=0.008. The sum of mean activation across time-window, within the composite “DMN” ROI, positively correlated with individuals' algorithmic complexity (pearson: r_{30}=0.379, p=0.036, CI=0.03 to 0.65, Figure 6h). Directly replicating previous studies [20,21], activation within the DMN ROI varied with learning (one-way anova: $F_{2,58}$=9.790, p<0.001, η_p^2=0.25) and was significantly increased in the last window, compared to the first (paired t-test: t_{30}=3.595, p=0.001, CI=-0.40 to -0.11, *d*=0.56, Figure 6i).

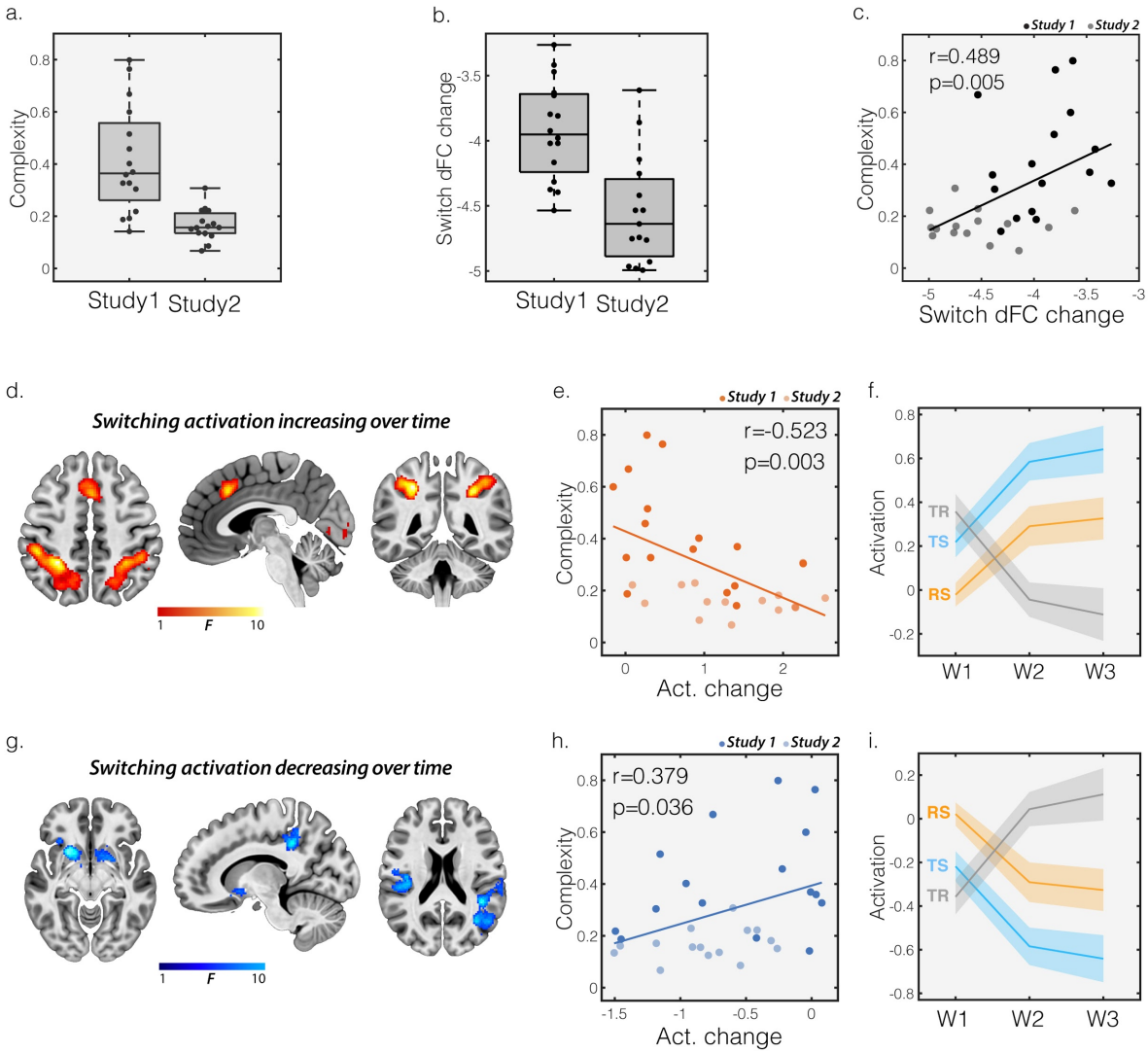

Figure 6. **Structuring behaviour is associated with greater redeployment of neural resources during learning.** a) Individuals algorithmic complexity compared between studies. b) Using the three time-windows defined in the RT analyses, the mean dynamic functional connectivity (dFC) change during switching, relative to trials, was calculated for each window and summed across windows (Switch dFC change, y-axis). Switch dFC change over time differed across studies with study 2 showing growing decreases in switching-dFC over time. c) Individuals switch dFC change positively correlated with algorithmic complexity. d) Main effect of time-window *F*-contrast maps showing regions where switching activation increased over time. e) The increase in the mean activation from regions identified in d, "MDC", over time-window (Act. change), negatively correlated with algorithmic complexity. f) Sampling trial activation in each time-window, using clusters identified in d, shows activation for trials decreasing over time-window (TR - trials, RS - rule-switching, TS - task-switching, W - window). g) Main effect of time-window *F*-contrast maps showing regions where switching activation decreased over time. h) The decrease in the mean activation from regions identified in g, over time-window, positively correlated with algorithmic complexity. h) Sampling trial activation in each time-window, using clusters identified in g, "DMN", shows activation for trials increasing over time-window.

Discussion

Overall, the results accord well with dynamic-network perspectives on the brain's functional organisation, but poorly with predictions from classic modular perspectives. Self-ordered switching (SOS) was associated with transient states of global dysconnectivity and widespread activation changes that were not specific to aPFC, as has been previously claimed. As individuals practiced the task, switching-dysconnectivity *deepened* and activation of frontoparietal regions was tuned toward switch vs. trial events. Furthermore, the scale of this change related to how much structure individuals applied to their behaviour. These findings accord with the hypothesis that cognitive control processes are emergent properties of dynamic network states. These results demonstrate that a fundamental property of the system is the concurrent optimisation of both behaviour and the resources that support behaviour with learning. More generally, the results highlight the value of cognitive paradigms that allow the participant sufficient latitude to structure their own behaviour.

One of the most striking results relates to the change in network dFC during switching. Previous studies have sought to map task-switching to the activity or connectivity of specific brain regions [28,76]. Here, when taking a more holistic view, we observed that switching involves a costly reconfiguration throughout the brain's functional connectome. This dynamic process of 'collapse and rebuild' (Figure 1) was marked by dysconnectivity and activation of distributed lateral frontoparietal cortices, subcortical and cerebellar regions, and the deactivation of the DMN.

This 'relaxation' of connectivity during switching complements previous work investigating the active states that are transiently formed when performing different tasks. Cognitive paradigms typically require task programs to be maintained so that stimuli inputs are appropriately computed to produce response outputs. Task program maintenance is typically associated with a stable high-connectivity state [44,62], where configurations of the brain's functional connectome are specific to the task at hand [22,47,63–65], and are more strongly expressed under greater cognitive load [22] or attentional focus [66]. The findings presented here indicate that SOS may involve a destabilisation of the task-state, whereby switches between task programs involve transient states characterised by rapid changes in regional activity that present as reductions in connectivity, as measured using correlational analyses.

Critically, the behavioural and neural markers of switching were not static, and were sensitive to learning. The costs to response speed that followed switching reduced as individuals learnt the demands of SOS. This may reflect a natural tendency towards efficiency [17] as individuals

were not explicitly instructed to speed up, or to respond as quickly as possible, but instead to try and gain as many points as they could .

Meanwhile, switching-dysconnectivity *deepened* with learning. This may reflect an optimised 'collapse and rebuild' process that more effectively 'clears the path' for the incoming task program to establish. These learning dynamics have broader implications; they may indicate that switch costs index different mixes of top-down cognitive controls [7] and bottom-up interference [4] depending on where an individual is on the learning curve. Switching processes may optimise as cognitive controls adapt to the demands of SOS and, therefore, minimise the interference between competing task programs.

Learning is a demanding process but this investment constructs task programs that benefit efficiency in the long term. Task programs are available for future recall and are further optimised with learning. This is apparent when learning new behaviours that have competing demands, e.g., car driving. In the absence of a task program, learning how to appropriately manage behaviour (e.g., pressing pedals) and attentional resources (e.g., monitoring speed, tracking surrounding vehicles) is cognitively demanding; however, being able to increasingly structure task programs, through learning, allows behaviour to increasingly automate and reduce cognitive demand, as fewer cognitive controls are required to guide behaviour on a moment-to-moment basis. Indeed, we observed improvements in behavioural performance as neural resources were redeployed toward switch vs trial events.

Specifically, activations in ACC and DLPC decreased for simple trial responses and *increased* for SOS events, as individuals learnt. Meanwhile, activation in posterior cingulate and putamen showed the opposing trend. This ongoing redeployment of neural resources may reflect the automation of the individual trial demands, with increasing focus on the SOS events where individuals are directly imposing structure to their behaviour.

Building on this, individuals varied in how much they structured their behaviour. Those most successful at the SOS paradigm were operating with a structured (low-complexity) task program. These individuals showed the most pronounced changes in brain function with learning. This was marked by greater increases in switching-dysconnectivity and greater changes in switching activation. Thus, individuals vary in their ability to create behaviourally efficient task programs and the most efficient show greater redeployment of their resources, toward a neural state that is more efficient.

Problems in forming, updating and switching between task programs may underlie the

difficulties with navigating daily life that pervade neuropsychiatric populations. Without being able to learn and rely on task programs to manage cognitive demands, each moment (attentional episode [58]) of daily life is compensated by expensive cognitive controls. Consider anxiety [77], depression [78], obsessive compulsive disorder [79] and autism spectrum disorders [80–82] where repetitive behaviours and rigid thought patterns are typical, or attention deficit hyperactivity disorder (ADHD) [83], neurodegeneration [84] and brain injury [62] where distractibility and goal-set maintenance is problematic. These symptoms may result from the suboptimal cognitive controls involved with creating, maintaining, updating or switching between task programs. Future research could benefit from incorporating self-ordered elements to studies of cognitive control in these clinical populations. Tapping the ability to efficiently organise behaviour may provide a clinical marker with high ecological validity.

A widely-held perspective is that cortical regions within aPFC are arranged along an abstract-concrete anterior-posterior axis [35,36]. Task-switching, as the exemplar of abstract processing, is often thought to be subserved by activities of the frontopolar cortices [8,28–30]. However, we and others have used instruction based learning [20,21], relation integration [46] and manipulations of task difficulty [57] and found distributed frontoparietal activation, with larger, and more anterior, portions of PFC active in contexts of rule novelty, high task difficulty and even during simple tasks that lack abstraction. This evidence provides an alternative view that cognitive demands promote recruitment of extended aPFC regions of a broader frontoparietal system.

Accordingly, the lack of activation differences in aPFC between task and rule switching, reported here, and indeed, a lack of a particularly strong activation profile for aPFC during switching, accords poorly with predictions of hierarchical models of PFC functional organisation; however, it is explainable from the multiple-demand view of frontoparietal activation. Task-switching paradigms typically enforce the tempo of individual trials and when switches occur. In these contexts, there can be greater cognitive demands as individuals are less able to structure their behaviour. They have to constantly adjust and respond to the environment. In contrast, the SOS paradigm used here, by definition, allows individuals to develop task programs that structure behaviour that mitigates cognitive demands.

Moving forward, we should consider the in-task learning that may occur during cognitive control studies. This may be an inevitable feature of cognition that will manifest even during simple procedures. Developing fMRI variants of paradigms that allow deeper hierarchical behavioural structures to be learnt should also be considered.

Finally, to build upon the generalisability of the present study, it will be important for future

studies to probe switches between tasks that tap different aspects of intelligence [85] and which systematically vary in similarity, as indexed by psychometric distance. There is some behavioural evidence that switch costs increase with the magnitude of the switch [86]; however, the neural mechanisms supporting switches of varying distance are yet to be characterised.

In summary, we developed a SOS paradigm that revealed switching to involve a widespread and metabolically costly reconfiguration of the brain's functional connectome that was characterised by a global state of dysconnectivity. The behavioural and neural markers of switching varied with learning and the extent to which individuals applied structure to their self-ordered behaviour. A fundamental property of human neurocognitive systems is the ongoing and concurrent self-optimisation of behavioural structure and network dynamics in order to maximise positive outcomes and minimise the use of neural resources.

Methods

Participants. There were 16 healthy volunteers (mean age 24.75 years, range 19-40, 10 female) in study 1 and 15 healthy volunteers (mean age 26.47 years, range 19-42, 11 female) in study 2. All volunteers were right-handed and gave written informed consent prior to participating. The University of Cambridge research ethics board approved the study protocol.

Self-ordered switch (SOS) paradigms. The SOS variants used in study 1 and 2 were composed of two visual discrimination tasks, a matching task (MT) and an odd one out (OOO) task, each with two rules, colour and shape (Figure 2). During MT trials, subjects were presented with a target and two probe objects (each defined by their shape and colour) and their task was to indicate which on the probes matched the target via a L/R button press. Similarly, OOO trials presented a 2x2 grid of objects and their task was to indicate which side of the screen contained the object that differed from the other 3. Subjects discriminated between objects based on the currently active rule. Responses to trials and switches between tasks or rules were indicated via an MR compatible button box that was held in the right hand.

In study 1, the paradigm used was designed to guide subject's switching behaviours with hierarchical feedback. Tasks were presented at the top and bottom of the display (Figure 2ai). The active task was denoted by a red border and the active rule with text in the middle of the task panel. A feedback panel was presented between each trial for 1.5s with 4 feedback bars, 1 for each condition (Figure 2aii), so subjects could track their progress on either task's sub-rules. In the centre of the display were additional feedback bars that tracked the progress made on either task and subject's overall score (Figure 2aiii). Overall score was calculated as the sum of differences between the task bars current and initial value. Filling both task bars resulted in a bonus of +10 points. Switching behaviour was encouraged as the inactive rule or task feedback bar was penalized if it was 3 or more points behind the active rule or task.

Thus, the objective was to first work on a task's sub-rules (Figure 2bi), and avoid penalties for dwelling in the same rule or task (Figure 2bii), to make progress on a task (Figure 2biii) and make progress on both tasks to receive the bonus points (Figure 2biv). When rule or task feedback bars reached their maximum value, they reset to the initial value (middle). Response errors decreased the feedback bar of the active condition. Therefore, those subjects who effectively structured their responses/time in each rule and task earned the most points.

The paradigm used in study 2 was designed to minimize the influence of feedback on the subjects switching behaviour. Instead of both tasks being shown simultaneously, only the

active task was on display (Figure 2c). The active rule was denoted in the same way with text in the centre of the display. The same tasks and rules were and responses were collected in the same way as in study 1. The feedback bars, penalties and bonus points were removed. The only feedback was the score at the top of the display which increased for correct responses. Response errors did not change the score. Within the task code, an internal 'switch criterion' was designed to stop the score from increasing if a subject had accrued a difference of 5 or more points between the two rules of the active task, or if a difference of 9 or more points had been accrued between the active rule or the active task and either of inactive task's rule conditions. In contrast to study 1, subjects participated in a 20 minute training session prior to scanning where they developed their own schema of how to effectively navigate between the tasks and rules.

Behavioural analysis. RT's were calculated as the time between the stimuli being presented to the display, or when a switch occurred, and the response being made. For each subject, correct responses were used to extract the median RT's for no switch trials and for the 1st trials following a task-switch or rule-switch. Similarly, response accuracy was calculated using the percentage of correct responses to no switch trials and the 1st trials following a task or rule-switch. The windowed analysis of RT split individuals' behavioural data into 1/3's and RT's were extracted in the same manner for each window.

Repetition bias was calculated to reflect the probability of the current trial condition being repeated. Specifically, the number of trial repeats was normalised by the total number of completed trials. A greater repetition bias reflects less switching events and a greater likelihood that an individual will repeat the condition on a given trial.

Algorithmic complexity. The degree to which subjects applied structure to their behaviour was indexed using algorithmic complexity. Here, we use the framework, outlined by [70], which combines a block decomposition method (BDM) and coding theorem method (CTM) [87] to provide a reasonable estimate of the Kolmorogov-Chaitin complexity (K) [88,89] of large strings in a computationally tractable way. The advantage of BDM is that it provides an estimate of K that not only considers statistical regularities, as captured by Shannon entropy, but is also sensitive to segments of an algorithmic nature. Behavioural timecourses were converted into a binary vector which represented the sequence of the 4 trial conditions performed by an individual. Sequence length naturally varied across individuals and to account for this we normalised an individual's algorithmic complexity by the mean algorithmic complexity calculated from 100 randomly shuffled versions of the individual's data (qualitatively similar

results were obtained without normalisation). NB:- as expected, the raw data showed a significantly lower complexity than the shuffled data (paired t-test: study 1 - t_{15}=-9.775, p<0.001, *d*=3.54; study 2 - t_{14}=-35.329, p<0.001, *d*=14.29).

MRI acquisition. Blood oxygenation level dependent (BOLD) fMRI recordings were made using a Siemens 3T Trim Trio scanner using the following parameters in both studies: repetition time (TR)=2s; echo time (TE)=30ms; Flip Angle=78°; 3mm^3 voxels; 3.75mm slice-gap; 32 axial slices. 630 volumes were acquired during the ~20-minute SOS task run. A T1-weighted magnetization prepared rapid acquisition gradient echo (MPRAGE) sequence was also acquired for each subject using the following parameters: TR=2250ms; TE=2.99ms; IT=900ms; Flip Angle=9°; 1mm^3 voxels, 256 axial slices.

Image data analysis. Image Pre-processing was conducted using standard parameters with the Statistical Parametric Mapping 12 (SPM)[1] toolbox in Matlab 2018b[2]. The first 10 volumes were discarded to account for T1-equilibrium effects. The remaining images were slice-time and motion-corrected, and the mean echo planar image (EPI) co-registered to the tissue segmented T1 image, normalised to 2mm^3 MNI space and spatial smoothing (full half width maximum = 8 mm kernel).

Subject level voxelwise modelling. Individuals voxelwise fMRI data was modelled using a General Linear Model (GLM) with the psychological events defined by responses to one of the 4 trial conditions (MT colour, MT shape, OOO colour, OOO shape), the 2 task-switches (MT to OOO, OOO to MT), 4 rule-switches (MT colour to MT shape, MT shape to colour, OOO colour to shape, OOO shape to colour) and the highly infrequent response errors. Models in study 1 included an additional set of events if rule or task bars de/incremented and if bonus points were awarded. These predictors were convolved with the canonical haemodynamic response function (HRF), durations were set to 0s. Individual's head motion and physiological nuisance variables were modelled using the 6 rigid-body realignment parameters, the mean timecourses from the white matter and cerebrospinal fluid (defined with individual's T1 anatomical segmentations with > 0.8 probability), their 1st order temporal derivatives, and additional spike regressors if framewise displacement[90] exceeded the voxel acquisition size (3mm). Beta maps for each psychological predictor were generated relative to the model intercept (constant).

Group level voxelwise modelling. Beta maps from the first-level fixed effects GLM were

[1] "SPM12 - Wellcome Trust Centre for Neuroimaging - UCL." Accessed July 30, 2019. https://www.fil.ion.ucl.ac.uk/spm/software/spm12/.

[2] "MATLAB - MathWorks - MATLAB & Simulink." Accessed July 30, 2019. https://www.mathworks.com/products/matlab.html.

assessed at the group-level with two random effects models. The first modelled trial events in a two-way task (MT, OOO) by rule (colour, shape) rm-anova. The second modelled the 2 task-switch and 4 rule-switch events in a one-way rm-anova. In all cases, a primary voxel statistical threshold of $p<0.01$ was applied, and the maps corrected for multiple comparisons at the cluster level using an FDR $p<0.05$ threshold. In cases where activation estimates were extracted for further analysis, a watershed transform[22] was applied to the FDR cluster-corrected group-level map to identify discrete clusters used to extract the mean beta weight across voxels from each subject.

Dynamic functional connectivity estimation. Generalised psychophysiological interaction (PPI) models [71,72] were fitted to pairwise to 159 regions of interest (ROI) defined by external atlases that encompassed the cortex, subcortex and cerebellum [73–75]. gPPI's were simultaneously estimated for the 4 trial and 6 switch events defined by a subject's 1st level model for each pair of ROIs using the following:

$$Y^T = \beta_0 + [Y^S * H(X)]\beta_G + [Y^S, H(X), E]\beta + e,$$

where, X, is the matrix of psychological timecourses and, $H(X)$, its HRF convolution. Y^T is the target ROI timecourse and, Y^S, the seed ROI timecourse. E is the matrix of motion & tissue signal timecourses. β_G are the gPPI betas weights, β, the beta weights of no-interest, β_0, is the model intercept and, e, the residual. The betas from each pair of ROIs were averaged and z-scored across condition.

Modelling learning effects. Individual's fMRI data were modelled to examine learning effects using predictors that captured trial responses and switch events for each of the three time-windows used in the RT analyses. In terms of connectivity, dFC was estimated for each connection, condition and time-window and then z-scored across condition and within each time-window. Changes in dFC across time-windows were summarised using the mean difference between switching and trials, across connection. This resulted in one value per time-window and individual. For activation, switching > trial contrasts were extracted each individual and time-window and modelled in a two-way rm-anova with study (two levels) as a between-subject factor and time-window (three levels) as a within-subject factor. Activation clusters showing the main effect of time-window were used to extract mean beta weights from each individual. The direction of the effect for each cluster was assessed using one-sample t-tests on the difference between activation in the 1st and last time-window.

Dice coefficient. Dice coefficients (DCE) were used to estimate spatial similarity of activation

maps between study 1 and study 2. Group level cluster-corrected activation maps were binarized dice coefficient calculated between each pairs of maps using the following formula:

$$DCE(A,B) = \frac{2(A \cap B)}{(A + B)}$$

Effect size calculations. *Partial eta squared* was used to calculate the proportion of variance explained for the main and interaction effects tested with anova models using the *F*-statistic and degrees of freedom by the following:

$$\eta_p^2 = \frac{(F * DF1)}{(F * DF1) + DF2}$$

Cohen's d was used to calculate the standard effect size of statistical comparisons by dividing the difference between two means by the pooled standard deviation, in the 2-sample case, or dividing the mean by the standard deviation in the 1-sample case, e.g.:

$$d = \frac{\underline{X}1 - \underline{X}2}{\sqrt{(SD_1^2 + SD_2^2) / 2}}$$

Code availability. Visual basic code used for the presentation of the SOS paradigms and Matlab code for conducting the data analyses are available upon request from the corresponding authors.

Data availability. Behavioural and pre-processed imaging data are available upon request from the corresponding authors.

Acknowledgements. This work was supported by funding to RED from the Engineering and Physical Sciences Research Council (EPSRC) via the centre for doctoral training (CDT) Neurotechnology programme at Imperial College London. The funders had no role in study design, data collection and analysis, decision to publish or preparation of the manuscript.

Author contributions. AH conceived and designed the self-ordered switching (SOS) paradigms and acquired the study data. RED analysed the data, created the figures and drafted the manuscript. GS and ES contributed analytical and visualisation tools. ES verified the data visualisation. AH, RL and PH verified analytical approaches. All authors provided interpretations of the findings and co-wrote the paper.

Competing interests. The authors declare no competing interests.

Reference

1. Culler, A. J. *Interference and Adaptability: An Experimental Study of Their Relation with Special Reference to Individual Differences*. (1912).
2. Jersild, A. T. *Mental Set and Shift*. (1927).
3. Spector, A. & Biederman, I. Mental Set and Mental Shift Revisited. *The American Journal of Psychology* vol. 89 669 (1976).
4. Allport, A., Styles, E. A. & Hsieh, S. Shifting intentional set: Exploring the dynamic control of tasks. in *Attention and performance XV: Conscious and nonconscious information processing* (eds. Umilta, C. & Moscovitch, M.) 421–452 (MIT Press, 1994).
5. Rubinstein, J., Meyer, D. E. & Evans, J. E. Executive Control of Cognitive Processes in Task Switching. *PsycEXTRA Dataset* (1994) doi:10.1037/e537272012-189.
6. Rogers, R. D. & Monsell, S. Costs of a predictible switch between simple cognitive tasks. *Journal of Experimental Psychology: General* vol. 124 207–231 (1995).
7. Meiran, N. Reconfiguration of processing mode prior to task performance. *Journal of Experimental Psychology: Learning, Memory, and Cognition* vol. 22 1423–1442 (1996).
8. Dove, A., Pollmann, S., Schubert, T., Wiggins, C. J. & von Cramon, D. Y. Prefrontal cortex activation in task switching: an event-related fMRI study. *Brain Res. Cogn. Brain Res.* **9**, 103–109 (2000).
9. Monsell, S. Task switching. *Trends Cogn. Sci.* **7**, 134–140 (2003).
10. Arrington, C. M. & Logan, G. D. The cost of a voluntary task switch. *Psychol. Sci.* **15**, 610–615 (2004).
11. Koch, I., Poljac, E., Müller, H. & Kiesel, A. Cognitive structure, flexibility, and plasticity in human multitasking—An integrative review of dual-task and task-switching research. *Psychological Bulletin* vol. 144 557–583 (2018).
12. Kiesel, A. *et al.* Control and interference in task switching--a review. *Psychol. Bull.* **136**, 849–874 (2010).
13. Arrington, C. M. & Logan, G. D. Voluntary task switching: chasing the elusive homunculus. *J. Exp. Psychol. Learn. Mem. Cogn.* **31**, 683–702 (2005).
14. Mayr, U. & Bell, T. On how to be unpredictable: evidence from the voluntary task-switching paradigm. *Psychol. Sci.* **17**, 774–780 (2006).
15. Lien, M.-C. & Ruthruff, E. Inhibition of task set: converging evidence from task choice in

the voluntary task-switching paradigm. *Psychon. Bull. Rev.* **15**, 1111–1116 (2008).
16. Kool, W., McGuire, J. T., Rosen, Z. B. & Botvinick, M. M. Decision making and the avoidance of cognitive demand. *J. Exp. Psychol. Gen.* **139**, 665–682 (2010).
17. Botvinick, M. M. & Cohen, J. D. The computational and neural basis of cognitive control: charted territory and new frontiers. *Cogn. Sci.* **38**, 1249–1285 (2014).
18. Petersen, S. E., van Mier, H., Fiez, J. A. & Raichle, M. E. The effects of practice on the functional anatomy of task performance. *Proceedings of the National Academy of Sciences* vol. 95 853–860 (1998).
19. Erika-Florence, M., Leech, R. & Hampshire, A. A functional network perspective on response inhibition and attentional control. *Nat. Commun.* **5**, 4073 (2014).
20. Hampshire, A. *et al.* Network mechanisms of intentional learning. *Neuroimage* **127**, 123–134 (2016).
21. Hampshire, A. *et al.* Probing cortical and sub-cortical contributions to instruction-based learning: Regional specialisation and global network dynamics. *Neuroimage* **192**, 88–100 (2019).
22. Soreq, E., Leech, R. & Hampshire, A. Dynamic network coding of working-memory domains and working-memory processes. *Nat. Commun.* **10**, 936 (2019).
23. Ruge, H., Schäfer, T. A., Zwosta, K., Mohr, H. & Wolfensteller, U. Neural representation of newly instructed rule identities during early implementation trials. *Elife* **8**, (2019).
24. Williams-Gray, C. H., Hampshire, A., Barker, R. A. & Owen, A. M. Attentional control in Parkinson's disease is dependent on COMT val158met genotype. *Brain* vol. 131 397–408 (2008).
25. Fallon, S. J., Williams-Gray, C. H., Barker, R. A., Owen, A. M. & Hampshire, A. Prefrontal dopamine levels determine the balance between cognitive stability and flexibility. *Cereb. Cortex* **23**, 361–369 (2013).
26. Parkin, B. *et al.* Dissociable Effects of Age and Parkinson's Disease on Instruction Based Learning. *PsyArXiv* (2020).
27. Matthews, P. M. & Hampshire, A. Clinical Concepts Emerging from fMRI Functional Connectomics. *Neuron* **91**, 511–528 (2016).
28. Koechlin, E., Basso, G., Pietrini, P., Panzer, S. & Grafman, J. The role of the anterior prefrontal cortex in human cognition. *Nature* **399**, 148–151 (1999).
29. Rushworth, M. F. S., Passingham, R. E. & Nobre, A. C. Components of switching intentional set. *J. Cogn. Neurosci.* **14**, 1139–1150 (2002).
30. Braver, T. S., Reynolds, J. R. & Donaldson, D. I. Neural mechanisms of transient and sustained cognitive control during task switching. *Neuron* **39**, 713–726 (2003).
31. Nelson, H. E. A modified card sorting test sensitive to frontal lobe defects. *Cortex* **12**, 313–324 (1976).
32. Reitan, R. M. & Wolfson, D. A selective and critical review of neuropsychological deficits and the frontal lobes. *Neuropsychol. Rev.* **4**, 161–198 (1994).
33. Shallice, T., Stuss, D. T., Picton, T. W., Alexander, M. P. & Gillingham, S. Multiple effects of prefrontal lesions on task-switching. *Front. Hum. Neurosci.* **1**, 2 (2007).
34. Roca, M. *et al.* Executive function and fluid intelligence after frontal lobe lesions. *Brain* **133**, 234–247 (2010).
35. Koechlin, E. & Summerfield, C. An information theoretical approach to prefrontal executive function. *Trends Cogn. Sci.* **11**, 229–235 (2007).
36. Badre, D. & D'Esposito, M. Is the rostro-caudal axis of the frontal lobe hierarchical? *Nat. Rev. Neurosci.* **10**, 659–669 (2009).
37. Mouraux, A., Diukova, A., Lee, M. C., Wise, R. G. & Iannetti, G. D. A multisensory investigation of the functional significance of the 'pain matrix'. *NeuroImage* vol. 54 2237–2249 (2011).
38. Yarkoni, T., Poldrack, R. A., Nichols, T. E., Van Essen, D. C. & Wager, T. D. Large-scale automated synthesis of human functional neuroimaging data. *Nat. Methods* **8**,

665–670 (2011).
39. Hampshire, A. & Sharp, D. J. Contrasting network and modular perspectives on inhibitory control. *Trends Cogn. Sci.* **19**, 445–452 (2015).
40. Lorenz, R., Hampshire, A. & Leech, R. Neuroadaptive Bayesian Optimization and Hypothesis Testing. *Trends in Cognitive Sciences* vol. 21 155–167 (2017).
41. Duncan, J. & Owen, A. M. Common regions of the human frontal lobe recruited by diverse cognitive demands. *Trends Neurosci.* **23**, 475–483 (2000).
42. Bassett, D. S. *et al.* Dynamic reconfiguration of human brain networks during learning. *Proc. Natl. Acad. Sci. U. S. A.* **108**, 7641–7646 (2011).
43. Cole, M. W. *et al.* Multi-task connectivity reveals flexible hubs for adaptive task control. *Nat. Neurosci.* **16**, 1348–1355 (2013).
44. Hellyer, P. J. *et al.* The control of global brain dynamics: opposing actions of frontoparietal control and default mode networks on attention. *J. Neurosci.* **34**, 451–461 (2014).
45. Gu, S. *et al.* Controllability of structural brain networks. *Nat. Commun.* **6**, 8414 (2015).
46. Parkin, B. L., Hellyer, P. J., Leech, R. & Hampshire, A. Dynamic network mechanisms of relational integration. *J. Neurosci.* **35**, 7660–7673 (2015).
47. Crittenden, B. M., Mitchell, D. J. & Duncan, J. Task Encoding across the Multiple Demand Cortex Is Consistent with a Frontoparietal and Cingulo-Opercular Dual Networks Distinction. *J. Neurosci.* **36**, 6147–6155 (2016).
48. Bassett, D. S. & Sporns, O. Network neuroscience. *Nat. Neurosci.* **20**, 353–364 (2017).
49. Khambhati, A. N., Medaglia, J. D., Karuza, E. A., Thompson-Schill, S. L. & Bassett, D. S. Subgraphs of functional brain networks identify dynamical constraints of cognitive control. *PLoS Comput. Biol.* **14**, e1006234 (2018).
50. Soreq, E., Violante, I., Daws, R. E. & Hampshire, A. Network sampling theory of intelligence. *Nat. Commun.*
51. Wager, T. D., Jonides, J. & Reading, S. Neuroimaging studies of shifting attention: a meta-analysis. *Neuroimage* **22**, 1679–1693 (2004).
52. Hampshire, A. & Owen, A. M. Fractionating attentional control using event-related fMRI. *Cereb. Cortex* **16**, 1679–1689 (2006).
53. Cusack, R., Mitchell, D. J. & Duncan, J. Discrete object representation, attention switching, and task difficulty in the parietal lobe. *J. Cogn. Neurosci.* **22**, 32–47 (2010).
54. Kim, C., Cilles, S. E., Johnson, N. F. & Gold, B. T. Domain general and domain preferential brain regions associated with different types of task switching: A Meta-Analysis. *Human Brain Mapping* vol. 33 130–142 (2012).
55. Crittenden, B. M., Mitchell, D. J. & Duncan, J. Recruitment of the default mode network during a demanding act of executive control. *Elife* **4**, e06481 (2015).
56. Kehagia, A. A. *et al.* Parsing the Roles of the Frontal Lobes and Basal Ganglia in Task Control Using Multivoxel Pattern Analysis. *J. Cogn. Neurosci.* **29**, 1390–1401 (2017).
57. Crittenden, B. M. & Duncan, J. Task difficulty manipulation reveals multiple demand activity but no frontal lobe hierarchy. *Cereb. Cortex* **24**, 532–540 (2014).
58. Duncan, J. The Structure of Cognition: Attentional Episodes in Mind and Brain. *Neuron* vol. 80 35–50 (2013).
59. Fedorenko, E., Duncan, J. & Kanwisher, N. Broad domain generality in focal regions of frontal and parietal cortex. *Proc. Natl. Acad. Sci. U. S. A.* **110**, 16616–16621 (2013).
60. Scott, G., Hellyer, P. J., Hampshire, A. & Leech, R. Exploring spatiotemporal network transitions in task functional MRI. *Human Brain Mapping* vol. 36 1348–1364 (2015).
61. Braun, U. *et al.* Brain state stability during working memory is explained by network control theory, modulated by dopamine D1/D2 receptor function, and diminished in schizophrenia. (2019) doi:10.1101/679670.
62. Hellyer, P. J., Scott, G., Shanahan, M., Sharp, D. J. & Leech, R. Cognitive Flexibility through Metastable Neural Dynamics Is Disrupted by Damage to the Structural

Connectome. *J. Neurosci.* **35**, 9050–9063 (2015).
63. Cox, D. D. & Savoy, R. L. Functional magnetic resonance imaging (fMRI) 'brain reading': detecting and classifying distributed patterns of fMRI activity in human visual cortex. *Neuroimage* **19**, 261–270 (2003).
64. Woolgar, A., Thompson, R., Bor, D. & Duncan, J. Multi-voxel coding of stimuli, rules, and responses in human frontoparietal cortex. *Neuroimage* **56**, 744–752 (2011).
65. Shirer, W. R., Ryali, S., Rykhlevskaia, E., Menon, V. & Greicius, M. D. Decoding subject-driven cognitive states with whole-brain connectivity patterns. *Cereb. Cortex* **22**, 158–165 (2012).
66. Rosenberg, M. D. *et al.* A neuromarker of sustained attention from whole-brain functional connectivity. *Nat. Neurosci.* **19**, 165–171 (2016).
67. Hampshire, A., MacDonald, A. & Owen, A. M. Hypoconnectivity and Hyperfrontality in Retired American Football Players. *Scientific Reports* vol. 3 (2013).
68. Rosa, M. J. *et al.* Sparse network-based models for patient classification using fMRI. *Neuroimage* **105**, 493–506 (2015).
69. Mason, S. L. *et al.* Predicting clinical diagnosis in Huntington's disease: An imaging polymarker. *Annals of Neurology* vol. 83 532–543 (2018).
70. Zenil, H. *et al.* A Decomposition Method for Global Evaluation of Shannon Entropy and Local Estimations of Algorithmic Complexity. *Entropy* vol. 20 605 (2018).
71. Friston, K. J. *et al.* Psychophysiological and modulatory interactions in neuroimaging. *Neuroimage* **6**, 218–229 (1997).
72. McLaren, D. G., Ries, M. L., Xu, G. & Johnson, S. C. A generalized form of context-dependent psychophysiological interactions (gPPI): a comparison to standard approaches. *Neuroimage* **61**, 1277–1286 (2012).
73. Buckner, R. L., Krienen, F. M., Castellanos, A., Diaz, J. C. & Yeo, B. T. T. The organization of the human cerebellum estimated by intrinsic functional connectivity. *J. Neurophysiol.* **106**, 2322–2345 (2011).
74. Fan, L. *et al.* The Human Brainnetome Atlas: A New Brain Atlas Based on Connectional Architecture. *Cerebral Cortex* vol. 26 3508–3526 (2016).
75. Schaefer, A. *et al.* Local-Global Parcellation of the Human Cerebral Cortex from Intrinsic Functional Connectivity MRI. *Cereb. Cortex* **28**, 3095–3114 (2018).
76. Charron, S. & Koechlin, E. Divided representation of concurrent goals in the human frontal lobes. *Science* **328**, 360–363 (2010).
77. Kashdan, T. B. & Rottenberg, J. Psychological flexibility as a fundamental aspect of health. *Clin. Psychol. Rev.* **30**, 865–878 (2010).
78. Fossati, P., Ergis, A. M. & Allilaire, J. F. [Executive functioning in unipolar depression: a review]. *Encephale* **28**, 97–107 (2002).
79. Chamberlain, S. R. *et al.* Orbitofrontal dysfunction in patients with obsessive-compulsive disorder and their unaffected relatives. *Science* **321**, 421–422 (2008).
80. Geurts, H. M., Corbett, B. & Solomon, M. The paradox of cognitive flexibility in autism. *Trends Cogn. Sci.* **13**, 74–82 (2009).
81. Watanabe, T. & Rees, G. Brain network dynamics in high-functioning individuals with autism. *Nat. Commun.* **8**, 16048 (2017).
82. Watanabe, T., Lawson, R. P., Walldén, Y. S. E. & Rees, G. A neuroanatomical substrate linking perceptual stability to cognitive rigidity in autism. *J. Neurosci.* (2019) doi:10.1523/JNEUROSCI.2831-18.2019.
83. Nigg, J. T. & Casey, B. J. An integrative theory of attention-deficit/ hyperactivity disorder based on the cognitive and affective neurosciences. *Dev. Psychopathol.* **17**, 785–806 (2005).
84. Kehagia, A. A., Barker, R. A. & Robbins, T. W. Revisiting the effects of Parkinson's disease and frontal lobe lesions on task switching: the role of rule reconfiguration. *J. Neuropsychol.* **8**, 53–74 (2014).

85. Daws, R. E. & Hampshire, A. The Negative Relationship between Reasoning and Religiosity Is Underpinned by a Bias for Intuitive Responses Specifically When Intuition and Logic Are in Conflict. *Front. Psychol.* **8**, 2191 (2017).
86. Arrington, C. M., Altmann, E. M. & Carr, T. H. Tasks of a feather flock together: similarity effects in task switching. *Mem. Cognit.* **31**, 781–789 (2003).
87. Lempel, A. & Ziv, J. On the Complexity of Finite Sequences. *IEEE Trans. Inf. Theory* **22**, 75–81 (1976).
88. Kolmogorov, A. N. Three approaches to the quantitative definition of information *. *Int. J. Comput. Math.* **2**, 157–168 (1968).
89. Chaitin, G. J. On the Length of Programs for Computing Finite Binary Sequences: statistical considerations. *J. ACM* **16**, 145–159 (1969).
90. Power, J. D., Barnes, K. A., Snyder, A. Z., Schlaggar, B. L. & Petersen, S. E. Spurious but systematic correlations in functional connectivity MRI networks arise from subject motion. *Neuroimage* **59**, 2142–2154 (2012).

Supplemental figures

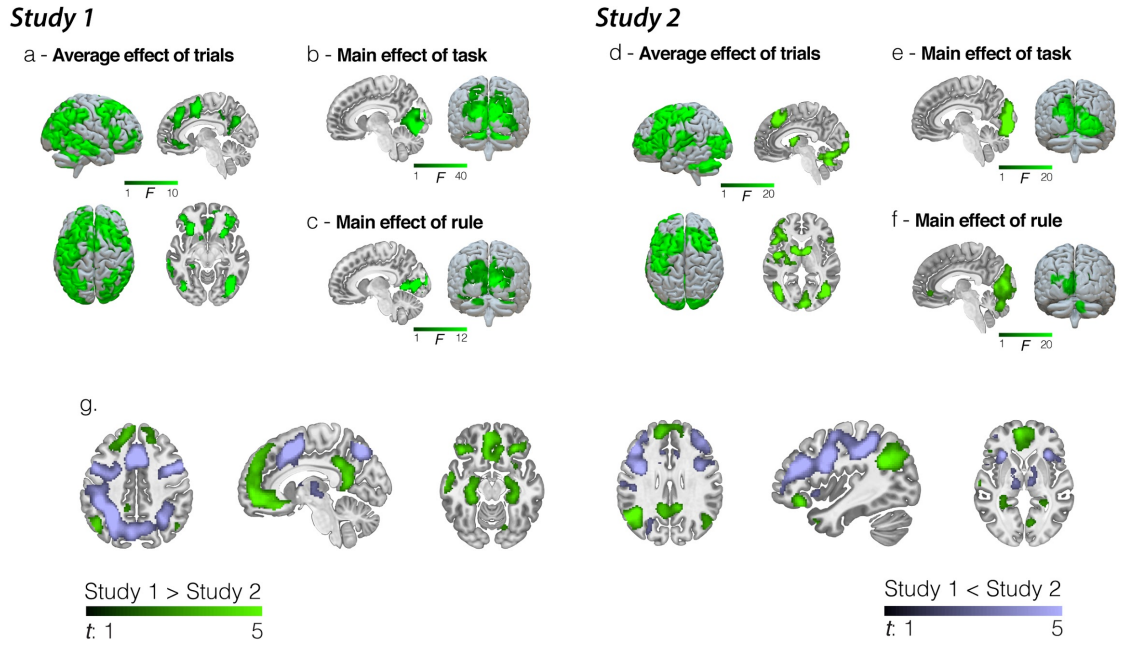

Supplemental Figure 1. **Trial response functional activation.** Study 1 - a) Activation *F*-contrasts for the average effect of trials (cluster extent k=268) & the main effects of task (b, k=329) & rule (c, k=6777). Study 2 - d) *F*-contrasts for the average effect of trials (k=559) & the main effects of task (e, k=606) & rule (f, k=442). g) Switch activation t-contrasts showing switch>trial contrast differences between studies (green=greater in study 1, melrose=lower in study 1). All statistical maps are thresholded at an uncorrected p<0.01 followed by a p<0.05 FDR cluster-correction.